

Optical Switching of Ion–Dipole Interactions in a Gramicidin Channel Analogue

Vitali Borisenko, Darcy C. Burns, Zhihua Zhang, and G. Andrew Woolley*

Contribution from the Department of Chemistry, University of Toronto, 80 St. George Street, Toronto, Ontario M5S 3H6, Canada

Received February 29, 2000

Abstract: Optical control of ion channel gating could permit the functional manipulation of excitable cells. We wished to examine the feasibility of using optical switching of ion–dipole interactions as a means of switching ion flux in channels. We prepared an analogue of the ion channel gramicidin A in which an azobenzene side chain was substituted for a valine side chain at position 1. The dipole moment of the azobenzene group can be reversibly switched between approximately 3 and 0 D by cis–trans photoisomerization. The observed conductance properties of the modified channels can be understood in terms of (switchable) ion–dipole interactions that control the height of the central barrier for Cs⁺ and Na⁺ movement through the pore. The predictable behavior of the system implies that larger dipole changes or changes closer to the central axis of the pore might effect complete gating.

Introduction

Optical methods have demonstrated utility for the investigation of physicochemical properties of biochemical systems.^{1–7} A photoregulated ion channel would extend the range of these investigations by enabling the direct manipulation of cellular excitability using light. A photoregulated ion transport system might, in principle,^{8–10} involve photoregulation of ion-binding sites,¹¹ positioning of channel-forming molecules in the membrane,^{12,13} creation of polar sites within the membrane,¹⁴ or direct alteration of the properties of ion channels.^{10,15–17}

The gramicidin channel is an attractive target for rational design because of its well-defined structural and functional properties under a wide range of conditions.¹⁸ In addition, its

relative simplicity makes chemical modification straightforward. Gramicidin dimers are formed by the association of two single-stranded β -helices, joined by intermolecular hydrogen bonds at their amino termini.^{19,20} Several photosensitive gramicidin analogues have been synthesized.^{13,16,17,21} Each of these employed an azobenzene derivative as the photochromic unit. This group is robust and undergoes reversible cis–trans photoisomerization without significant photobleaching.²² The wavelengths required (>330 nm) do not cause photodegradation of gramicidin Trp residues.²³

Optical modulation of the insertion of a gramicidin into bilayers has been reported with a C-terminal azobenzene-based modification.¹³ Covalently linked dimers of gramicidin have also been reported, in which an azobenzene group forms part of the linker.^{16,17} Although effects of photoisomerization on channel activity were observed in these cases, a straightforward interpretation of activity in structural terms was not possible. Previously, we reported the modification of the C-terminal end of gramicidin with an alkylamino-azobenzene moiety. This derivative showed photosensitive blocking of the entrance and exit of the gramicidin channel.^{21,24} Although the photomodulation could be understood in structural terms, significant redesign of the C-terminus of the peptide would be required for very large changes in conductance to be obtained.

In view of recent results supporting an important role for ion–dipole interactions in controlling conductance in gramicidin channels^{25–29} and in cation channels generally,^{30,31} we wished

* Corresponding author. Tel./fax: 416-978-0675. E-mail: awoolley@chem.utoronto.ca.

(1) Willner, I.; Rubin, I. *Angew. Chem., Int. Ed. Engl.* **1996**, *35*, 367–385.

(2) Ulysse, L.; Cubillos, J.; Chmielewski, J. *J. Am. Chem. Soc.* **1995**, *117*, 8466–8467.

(3) Kumita, J. R.; Smart, O. S.; Woolley, G. A. *Proc. Natl. Acad. Sci. U.S.A.* **2000**, *97*, 3803–3808.

(4) Adams, S. R.; Tsien, R. Y. *Annu. Rev. Physiol.* **1993**, *55*, 755–784.

(5) Nerbonne, J. M. *Curr. Opin. Neurobiol.* **1996**, *6*, 379–386.

(6) Politz, J. C. *Trends Cell. Biol.* **1999**, *9*, 284–287.

(7) Curley, K.; Lawrence, D. S. *Curr Opin. Chem. Biol.* **1999**, *3*, 84–88.

(8) Fyles, T. M.; Suresh, V. V. *Can. J. Chem.* **1994**, *72*, 1246–1253.

(9) Fyles, T. M. *Curr. Opin. Chem. Biol.* **1997**, *1*, 497–505.

(10) Bayley, H. *Curr. Opin. Biotechnol.* **1999**, *10*, 94–103.

(11) Shinkai, S. In *Bioorganic Chemistry Frontiers*; Dugas, H., Ed.; Springer-Verlag: Berlin, 1990; Vol. 1, pp 161–195.

(12) Ueda, T.; Nagamine, K.; Kimura, S.; Imanishi, Y. *J. Chem. Soc., Perkin Trans. 2* **1995**, 365–368.

(13) Osman, P.; Martin, S.; Milojevic, D.; Tansey, C.; Separovic, F. *Langmuir* **1998**, *14*, 4238–4242.

(14) Anzai, J.; Osa, T. *Tetrahedron* **1994**, *50*, 4039–4070.

(15) Chang, C. Y.; Niblack, B.; Walker, B.; Bayley, H. *Chem. Biol.* **1995**, *2*, 391–400.

(16) Stankovic, C. J.; Heinemann, S. H.; Schreiber, S. L. *Biochim. Biophys. Acta* **1991**, *1061*, 163–170.

(17) Sukhanov, S. V.; Ivanov, B. B.; Orekhov, S. Y.; Barsukov, L. I.; Arseniev, A. S. *Biol. Membr.* **1993**, *10*, 535–542 (in Russian).

(18) Koeppe II, R. E.; Andersen, O. S. *Annu. Rev. Biophys. Biomol. Struct.* **1996**, *25*, 231–258.

(19) Andersen, O. S. *Annu. Rev. Physiol.* **1984**, *46*, 531–548.

(20) Woolley, G. A.; Wallace, B. A. *J. Membr. Biol.* **1992**, *129*, 109–136.

(21) Lien, L.; Jaikaran, D. C. J.; Zhang, Z.; Woolley, G. A. *J. Am. Chem. Soc.* **1996**, *118*, 12222–12223.

(22) Rau, H. In *Photochromism. Molecules and Systems*; Durr, H.; Bouas-Laurent, H., Eds.; Elsevier: Amsterdam, 1990; pp 165–192.

(23) Busath, D. D.; Hayon, E. *Biochim. Biophys. Acta* **1988**, *944*, 73–78.

(24) Woolley, G. A.; Zunic, V.; Karanicolas, J.; Jaikaran, A. S.; Starostin, A. V. *Biophys. J.* **1997**, *73*, 2465–2475.

(25) Andersen, O. S.; Greathouse, D. V.; Providence, L. L.; Becker, M. D.; Koeppe, R. E., II. *J. Am. Chem. Soc.* **1998**, *120*, 5142–5146.

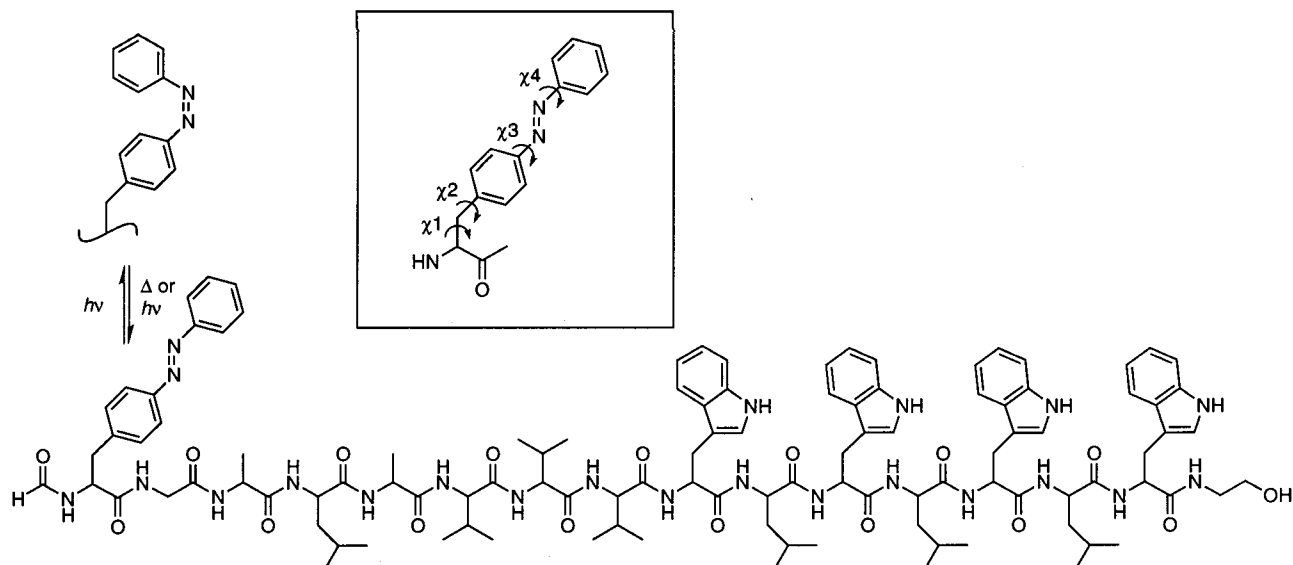


Figure 1. Chemical structure of phenylazo-phenylalanine (Pap¹)-gramicidin A. (Inset) Pap side-chain torsion angle designations.

to test the possibility of channel photoregulation via dipole switching. Detailed studies of the effects of side-chain dipoles on the function of gramicidin channels have been performed by several groups.^{25,29,32,33} Even though gramicidin side chains are not in direct contact with the permeating ion, channel properties can be strongly affected by the position and magnitude of side-chain dipole moments. Efforts have been focused on understanding the effects of Trp side-chain dipole moments on conductance (at positions Trp⁹, Trp¹¹, Trp¹³, Trp¹⁵)^{26–29,34,35} and the effects of side-chain dipole moment changes at position 1 of the channel (in the center of the membrane).^{36–39} Given the well-defined structure of the gramicidin channel, the effects of these dipoles can be discussed with reference to specific orientations of side-chain dipoles relative to the ion permeation pathway. The results of all these studies have been rationalized in terms of through-space ion–dipole interactions.^{25,29,32,33,36}

We decided to focus on dipole switching at position 1, since, under many conditions, ion translocation is rate limiting in the gramicidin channel so that electrostatic changes near the center of the membrane might be expected to have the largest effects on conductance.^{19,36} For instance, the single-channel sodium

conductance decreased 10-fold when hexafluorovaline (side-chain dipole, +1.6 D) was substituted for valine (side-chain dipole, –0.4 D) at position 1.³⁷

There is a significant dipole moment change associated with trans-to-cis isomerization of azobenzene (0–3 D).²² We therefore prepared a gramicidin derivative in which valine at position 1 was replaced by phenylazo-phenylalanine (Pap, Figure 1). We find that photoisomerization of Pap¹-gA(trans) to Pap¹-gA(cis) causes conductance changes that can be understood in terms of an increase in the central barrier for Cs⁺ and Na⁺ translocation via an ion–dipole interaction.

Materials and Methods

N-Fmoc-*p*-amino-phenylalanine (Fmoc = 9-fluorenylmethyl-oxy-carbonyl) was obtained from Bachem (King of Prussia, PA). Diphtanoyl-phosphatidylcholine was purchased from Avanti Polar Lipids Inc. (Alabaster, AL). Gramicidin, decane, CsCl, NaCl, HCl, TEA, and the buffer *N,N*-bis(2-hydroxyethyl)-2-aminoethanesulfonic acid (BES) were obtained from Sigma Aldrich Canada (Oakville, ON).

Synthesis. The preparation of gramicidin in which the valine at position 1 is replaced by phenylazo-phenylalanine (Pap¹-gA) followed the semisynthetic procedure described by Weiss and Koeppe⁴⁰ and Morrow et al.^{38,41} for the preparation of other position 1 mutants of gramicidin.

(i) Preparation of Fmoc-Pap. Fmoc-protected Pap was prepared via a modification of the procedure we described previously.⁴² *N*-Fmoc-*p*-amino-phenylalanine (1.9 g, Bachem) was combined with 1.5 equiv of nitrosobenzene (Aldrich) in 150 mL of glacial acetic acid and stirred at room temperature overnight. The reaction mixture was poured into 900 mL of cold water, and the pH was adjusted to 4 with sodium bicarbonate. The brown precipitate was washed with water and then redissolved in 90 mL of THF. The solution was cooled on ice, and cold water was added slowly (approximately 60 mL) until a precipitate formed. This procedure was repeated two more times to yield 1.1 g of Fmoc-Pap as a yellow-orange solid (yield 47%). TLC (EtOAc/PE/MeOH 3:2:2.8): *R*_f = 0.7. High-resolution FABMS: MH⁺ C₃₀H₂₆N₃O₄, calcd 492.1923, found 492.1928.

(ii) Preparation of Fmoc-Pap¹-Gramicidin. Fmoc-Pap (15.2 mg) was mixed with 1 equiv of *O*-(7-azabenzotriazol-1-yl)-*N,N,N',N'*-tetramethyluronium hexafluorophosphate (HATU) and 2 equiv of

(26) Busath, D. D.; Thulin, C. D.; Hendershot, R. W.; Phillips, L. R.; Maughan, P.; Cole, C. D.; Bingham, N. C.; Morrison, S.; Baird, L. C.; Hendershot, R. J.; Cotten, M.; Cross, T. A. *Biophys. J.* **1998**, *75*, 2830–2844.

(27) Cotten, M.; Tian, C.; Busath, D. D.; Shirts, R. B.; Cross, T. A. *Biochemistry* **1999**, *38*, 9185–9197.

(28) Dorigo, A. E.; Anderson, D. G.; Busath, D. D. *Biophys. J.* **1999**, *76*, 1897–1908.

(29) Phillips, L. R.; Cole, C. D.; Hendershot, R. J.; Cotten, M.; Cross, T. A.; Busath, D. D. *Biophys. J.* **1999**, *77*, 2492–2501.

(30) Chung, S. H.; Allen, T. W.; Hoyle, M.; Kuyucak, S. *Biophys. J.* **1999**, *77*, 2517–2533.

(31) Roux, B.; MacKinnon, R. *Science* **1999**, *285*, 100–102.

(32) Benamar, D.; Daumas, P.; Trudelle, Y.; Calas, B.; Bennes, R.; Heitz, F. *Eur. Biophys. J.* **1993**, *22*, 145–150.

(33) Hu, W.; Cross, T. A. *Biochemistry* **1995**, *34*, 14147–14155.

(34) Becker, M. D.; Greathouse, D. V.; Koeppe, R. E., II; Andersen, O. S. *Biochemistry* **1991**, *30*, 8830–8839.

(35) Daumas, P.; Benamar, D.; Heitz, F.; Ranjalay-Rasoloarijao, L.; Mouden, R.; Lazaro, R.; Pullman, A. *Int. J. Pept. Protein Res.* **1991**, *38*, 218–228.

(36) Koeppe, R. E., II; Mazet, J. L.; Andersen, O. S. *Biochemistry* **1990**, *29*, 512–520.

(37) Barrett Russell, E. W.; Weiss, L. B.; Navetta, F. I.; Koeppe, R. E., II; Andersen, O. S. *Biophys. J.* **1986**, *49*, 673–686.

(38) Morrow, J. S.; Veatch, W. R.; Stryer, L. *Biophys. J.* **1978**, *17*, 26a.

(39) Russell, E. W.; Weiss, L. B.; Navetta, F. I.; Koeppe, R. E., II; Andersen, O. S. *Biophys. J.* **1986**, *49*, 673–686.

(40) Weiss, L. B.; Koeppe, R. E., II. *Int. J. Pept. Protein Res.* **1985**, *26*, 305–310.

(41) Morrow, J. S.; Veatch, W. R.; Stryer, L. *J. Mol. Biol.* **1979**, *132*, 733–738.

(42) Liu, D.; Karanicolas, J.; Yu, C.; Zhang, Z.; Woolley, G. A. *Bioorg. Med. Chem. Lett.* **1997**, *7*, 2677–2680.

diisopropylethylamine (DIPEA) in 1.2 mL of dry DMF, and then the mixed solution was added dropwise to 49 mg (0.9 equiv) of des-(formylvalyl)-gramicidin (prepared exactly as described in ref 40) over 5 min. The reaction mixture was stirred at room temperature for 3 h, and then the solvent was removed under high vacuum. The product was dissolved in 1 mL of methanol and loaded onto an LH-20 gel filtration column running in methanol. The fractions containing product, as identified by their UV spectra, were combined, and the methanol was removed to give Fmoc-Pap¹-gramicidin as an orange solid. $R_f = 0.8$ (chloroform/methanol/water (CMW) 65:25:4). MS(ES): $[\text{MH}^+]$ $\text{C}_{123}\text{H}_{155}\text{N}_{22}\text{O}_{18}$, calcd 2229.7, obsd 2229.

(iii) Preparation of Pap¹-Gramicidin. Fmoc-Pap¹-gramicidin (65.9 mg) was dissolved in 0.8 mL of dry DMF, and then 1.5 mL of 20% piperidine in DMF was added dropwise. The reaction mixture was stirred at room temperature overnight, and then DMF and piperidine were removed under high vacuum. The solid was dissolved in 1 mL of MeOH and again loaded onto an LH-20 gel filtration column. The fractions containing product, as identified by their UV spectra, were pooled and concentrated to give 30 mg of a yellow solid. $R_f = 0.78$ (CMW 65:25:4). MS(ES): $[\text{MH}^+]$ $\text{C}_{108}\text{H}_{145}\text{N}_{22}\text{O}_{16}$, calcd 2007.5, obsd 2007.

(iv) Preparation of Formic–Acetic Anhydride. Formic acid (2.5 mL) was added dropwise to 5 mL of cooled acetic anhydride with stirring. The reaction mixture was heated to 50 °C for 15 min with stirring and then allowed to cool and stored in a refrigerator.

(v) Preparation of *N*-Formyl-Pap¹-Gramicidin. Pap¹-gramicidin (30 mg) was dissolved in 2 mL of THF and cooled in ice water. The pH of the reaction mixture was adjusted from 5 to 7 by adding 1 drop of TEA, and then 25 μL of formic–acetic anhydride was added. The reaction mixture was allowed to warm to room temperature and then stirred at room temperature for 2 h. The solvent was removed under high vacuum to give an orange product that was redissolved in 1 mL of methanol and then purified twice by HPLC. The HPLC conditions were as follows: Zorbax C-8 column, isocratic conditions, 88% methanol/12% water, flow rate 1.2 mL/min (retention time 6 min). $R_f = 0.76$ (CMW 65:25:4). MS(ES): $[\text{MH}^+]$ $\text{C}_{109}\text{H}_{145}\text{N}_{22}\text{O}_{17}$, calcd 2035.5, obsd 2034.9; MNa^+ 2056.8. Purity as estimated by HPLC was greater than 98%.

Single-Channel Measurements. The general techniques for single-channel recording of gramicidin channels have been described previously.⁴³ Peptides (~10 nM in MeOH) were added to membranes formed from diphytanoyl-phosphatidylcholine/decane (50 mg/mL). The trans state of Pap was obtained by dark adaptation of a stock solution of the peptide in MeOH. Photoisomerization to the cis state was achieved by irradiation of the stock solution with a nitrogen laser ($\lambda = 337$ nm; 150 $\mu\text{J}/\text{pulse}$; 1.5 ns/pulse/15 Hz) for ~1 h. Although isomerization in situ is also possible with our experimental arrangement,²¹ isomerization of stock solutions was performed to permit monitoring of the *cis*-azobenzene content by UV absorbance spectroscopy. Lipid bilayers were formed across a ~100- μm hole in a polypropylene pipet tip by painting a solution of lipid in decane. The pipet tip was mounted in a Teflon cell through a small hole in the back face. The front face of this cell had a removable circular glass window. Silver/silver chloride electrodes were placed in the pipet tip and in a cylindrical well drilled from the top of cell. Symmetrical, buffered (5 mM BES, pH 7) CsCl (1 or 0.1 M), NaCl (1 M), or HCl (0.1 M, unbuffered) solutions were used. All measurements were made at room temperature.

The current through lipid bilayers containing the gramicidin derivatives was measured, and the voltage was set using an Axopatch 1D patch-clamp amplifier (Axon Instruments) controlled by Synapse (Synergistic Research Systems) software. Single-channel events were recorded for a period of several hours for each set of experimental conditions. Data were filtered at 50 or 100 Hz, sampled at 1 kHz, stored directly to disk, and analyzed using Synapse and Igor (Wavemetrics, Inc.) software. Mean lifetimes and current amplitudes were determined by manual fitting of appropriate functions to the corresponding histograms using the program Mac-Tac (Version 2.0, Instrutech Corp.).

Molecular Modeling. All molecular modeling was performed on a Silicon Graphics Octane system (Irix 6.4) using Spartan (SGI version 5.0.3) and HyperChem (SGI version 4.5) software packages.

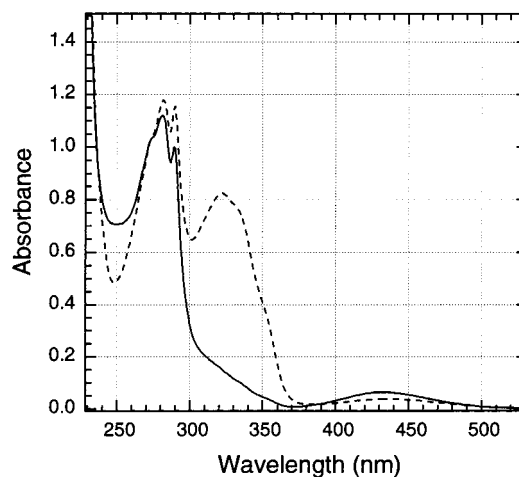


Figure 2. UV spectra of dark-adapted (*trans*) Pap¹-gA (---) and photoirradiated Pap¹-gA (—) in methanol.

The gramicidin channel structure, taken as a starting point for conformational energy and electrostatic calculations, was obtained from the Protein Data Bank (PDB code 1MAG). A single Na^+ ion was positioned in the center of the channel. Calculations were performed using the Amber force field⁴⁴ within the HyperChem molecular modeling package. Before calculations could begin, the Pap residue had to be parametrized for use with the force field. Separate parameters were developed for *cis* and *trans* conformations of Pap. Equilibrium bond lengths and angles were taken from the corresponding X-ray structures.^{45,46} Atom-centered partial charges were calculated using ab initio methods on the model compound *N*-acetyl-*N'*-methyl-phenylazophenylalanine carboxamide. This compound was built in Spartan, and χ_3 and χ_4 torsion angles (Figure 1) were adjusted to either (a) +57°, +57°, (b) -57°, -57°, (c) +123°, +123°, or (d) -123°, -123°, to produce the four expected low-energy conformers of *cis*-Pap, each of which has a different set of partial charges. These angles (χ_3 and χ_4) were set to 0° for *trans*-Pap. The angles χ_1 and χ_2 were set at -60° and +100° throughout. Single-point energy Hartree–Fock ab initio calculations were performed on each of these molecules using the 6-31G* basis set. Partial charges were then assigned using the electrostatic potential fitting algorithm within Spartan.

Conformational energy as a function of χ_1 and χ_2 was calculated using HyperChem (with the Amber force field) for each of the four different *cis*-Pap conformations. The angles χ_1 and χ_2 were each rotated through 360° in 4-deg increments, and single-point energies were calculated. A constant dielectric ($\epsilon = 5$) was used with no nonbonded cutoffs, and 1–4 scale factors were set at 0.5. Electrostatic interaction energies between the Pap partial charges and the Na^+ ion were calculated for each conformation by removing the rest of the molecule and setting the partial charges of backbone and β - CH_2 group atoms of the Pap residue to zero. Side-chain dipole moments were calculated and represented in Grasp (v.1.2)⁴⁷ on the basis of the assigned partial charges.

Results

The gramicidin analogue Pap¹-gA (Figure 1) was synthesized via replacement of Val¹ in natural gramicidin A using a modification of the procedure described by Weiss and Koeppel.⁴⁰ Figure 2 shows UV–vis spectra of Pap¹-gA in methanol in dark-adapted (*trans*) and photoirradiated (predominantly *cis*)²¹ states. As expected,²² the azobenzene π – π^* band (330 nm) decreased in intensity upon irradiation, the n – π^* band (430 nm) increased, and the Trp absorption (280, 290 nm) was essentially unaffected.

(44) Cornell, W. D.; Cieplak, P.; Bayly, C. I.; Gould, I. R.; Merz, K. M., Jr.; Ferguson, D. M.; Spellmeyer, D. C.; Fox, T.; Caldwell, J. W.; Kollman, P. A. *J. Am. Chem. Soc.* **1995**, *117*, 5179–5197.

(45) Hampson, G. C.; Robertson, J. M. *J. Chem. Soc.* **1941**, 409–413.

(46) Brown, C. J. *Acta Crystallogr.* **1966**, *21*, 146–152.

(47) Nicholls, A.; Sharp, K. A.; Honig, B. *Proteins* **1991**, *11*, 281–296.

(43) Busath, D.; Szabo, G. *Biophys. J.* **1988**, *53*, 689–695.

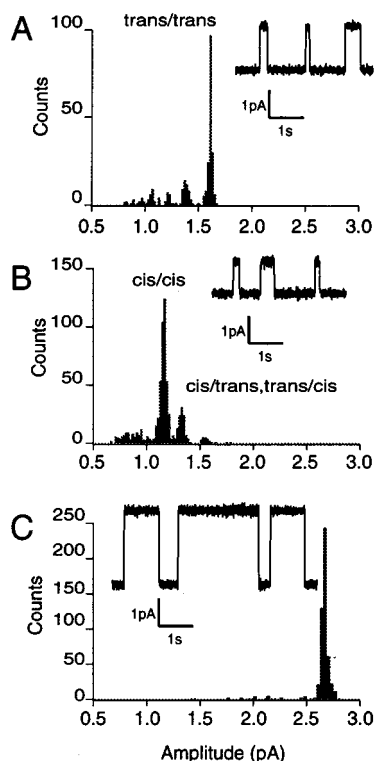


Figure 3. Single-channel current amplitude histograms and representative single-channel events (inset) of dark-adapted (trans) Pap¹-gA (A), extensively photoirradiated Pap¹-gA (predominantly Pap¹-gA(cis/cis)) (B), and native gA (C). The currents were obtained at +200 mV, 1.0 M NaCl, 5 mM BES, pH 7, DPhPC/decane membranes; filtering was at 100 Hz. Several hundred channels of each type were characterized.

Table 1. Functional Properties of Pap¹-gA Channels^a

channel type	1 M NaCl		1 M CsCl		0.1 N HCl	
	Λ	τ	Λ	τ	Λ	τ
gA	13	1.18	46	0.43	170	0.17
Pap ¹ -gA(trans/trans)	8	0.30	34	0.23	160	0.06
Pap ¹ -gA(cis/trans)	6.5		31.5			
Pap ¹ -gA(cis/cis)	6	0.22	29	0.11	172	0.06
hybrid gA/Pap ¹ -gA(trans)			40	0.27		
hybrid gA/Pap ¹ -gA(cis)			38	0.23		

^a Λ , single-channel conductance (pS) measured at 200 mV; τ , single-channel mean lifetime (s) measured at 200 mV.

The cis state is relatively stable; it reverts to the trans state with a half-life (in the dark) of >10 h at room temperature in methanol or saline solution (pH 7.0) and >2 h in 0.1 N HCl.

Effects of Photoirradiation on Single-Channel Currents. Single-channel recordings of Pap¹-gA with 1 M NaCl as the electrolyte and an applied potential of 200 mV are shown in Figure 3. Dark-adapted Pap¹-gA channels (Figure 3A) exhibit about 60% of the conductance of native gA (Figure 3C) under these conditions. The mean lifetimes are similar; the lifetime of Pap¹-gA(trans) is 0.3 s, whereas that of native gA is 1.2 s (Table 1). Irradiation of dark-adapted Pap¹-gA leads to the formation of Pap¹(cis)-gA (Figure 3B). The presence of both Pap¹(trans)-gA and Pap¹(cis)-gA in the membrane can, in principle, lead to conducting dimers of four types: trans/trans, cis/trans, trans/cis, and cis/cis. In the present case, three different levels of current were distinguished: 1.2, 1.3, and 1.6 pA. The 1.6 pA level corresponds to the dark-adapted, and therefore, the trans/trans state. The relative abundance of the 1.2 and 1.3 pA levels was dependent on the time of exposure to 337 nm light. With extensive irradiation, only the 1.2 pA level was seen. Therefore, we assign this level to the cis/cis channel and the

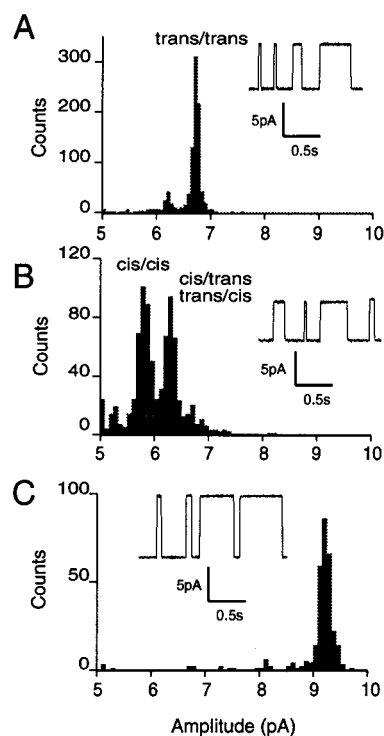


Figure 4. Single-channel amplitude histograms and representative single-channel events (inset) of dark-adapted (trans) Pap¹-gA (A), photoirradiated Pap¹-gA (a mixture of Pap¹-gA(cis/cis) and Pap¹-gA(cis/trans;trans/cis channels) (B), and native gA (C). The currents were obtained at +200 mV, 1.0 M CsCl, 5 mM BES, pH 7, DPhPC/decane membrane; filtering was at 100 Hz. Several hundred channels of each type were characterized.

1.3 pA level to a superposition of the trans/cis and cis/trans channels (vide infra). The changes in conductance of Pap¹-gramicidin channels seen upon photoirradiation at 337 nm are reversible upon exposure to broad spectrum longer-wavelength light; i.e., one observes a decrease in the frequency of appearance of cis/cis channels with a consequent increase in the occurrence of cis/trans, trans/cis, and trans/trans channels. The lifetimes of all these states are similar to one another as well as to those of native gA channels (Table 1).

Figure 4 shows single-channel recordings of Pap¹-gA with 1 M CsCl as the electrolyte and an applied voltage of 200 mV. A pattern is observed similar to that with the NaCl solution except that the differences in conductance between the states are smaller fractions of the total conductance.

Single-Channel Current–Voltage (*I*–*V*) Relationships. The shape of the single-channel current–voltage (*I*–*V*) relationship depends on the potential profile experienced by ions as they cross the membrane field.^{26,48} At high permeant ion concentrations (e.g., 1 M NaCl or 1 M CsCl), with diphytanoyl-phosphatidylcholine membranes, ion translocation through the pore is believed to be rate limiting.^{28,49–51} If a modification of the channel at the center of the membrane were to increase the barrier for translocation, an increase in the superlinearity of the *I*–*V* curve would be expected to result.³⁷

The curvature of *I*–*V* plots is best visualized by plotting normalized conductance (i.e., the conductance measured at voltage *V* divided by the conductance measured at 25 mV)

(48) Hladky, S. B.; Haydon, D. A. *Biochim. Biophys. Acta* **1972**, *274*, 294–312.

(49) Becker, M. D.; Koeppe, R. E., II; Andersen, O. S. *Biophys. J.* **1992**, *62*, 25–27.

(50) Andersen, O. S. *Biophys. J.* **1983**, *41*, 147–165.

(51) Hladky, S. B. *Novartis Found. Symp.* **1999**, *225*, 93–107.

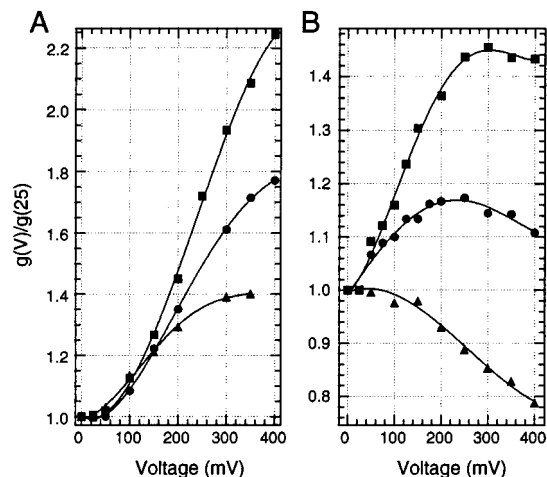


Figure 5. Plots of normalized conductance versus voltage. (A) 1 M NaCl; (B) 1 M CsCl. Pap¹-gA(cis/cis) (■), Pap¹-gA(trans/trans) (●), and native gA (▲). All solutions contained 5 mM BES, pH 7; filtering was at 50 or 100 Hz.

versus voltage. Figure 5 shows $g(V)/g(25)$ versus voltage curves observed with 1 M NaCl (Figure 5A) and 1 M CsCl (Figure 5B) as the electrolyte. With NaCl, the ratio $g(V)/g(25)$ is greater than or equal to 1 at all voltages; however, the values of $g(V)/g(25)$ are always larger for Pap¹-gA(trans/trans) than for gA and always larger for Pap¹-gA(cis/cis) than for Pap¹-gA(trans/trans). That is, Pap¹-gA(cis/cis) gives the most superlinear $I-V$ curve. The same pattern is observed with CsCl, except that at high voltages the ratio $g(V)/g(25)$ begins to decrease, indicating that a process other than translocation becomes rate limiting (since the gramicidin channel is saturable, the ratio $g(V)/g(25)$ must ultimately tend to zero). The voltage at which the ratio begins to decline is noticeably higher for Pap¹-gA(cis/cis) (~300 mV) than for Pap¹-gA(trans/trans) (~200 mV) than for gA (50 mV).

At very low permeant ion concentrations and high applied voltages, ion entry into the channel becomes rate limiting.^{50,52,53} Under these conditions, changes to the channel in the center of the membrane are expected to have little effect on conductance.³⁷ Figure 6 shows single-channel $I-V$ curves obtained in 0.1 M CsCl for gA, and for Pap¹-gA in trans/trans and cis/cis forms. Nonpermeant triethylammonium chloride (0.4 M) was added to minimize interfacial polarization effects.^{19,53} As the voltage is increased, all the currents tend to the same limiting value ($\sim 2 \pm 0.2$ pA) at +400 mV.

Hybrid Channels. As a further probe of the structural and functional effects of a valine to phenylazo-phenylalanine substitution at position 1, we investigated the ability of Pap¹-gA peptides to form hybrid channels with native gA peptides. Figure 7 shows current amplitude histograms obtained when Pap¹-gA(cis) and native gA were added simultaneously to membranes with 1 M CsCl as the electrolyte. In addition to the single-channel currents expected for Pap¹-gA(cis/cis) homodimers and gA homodimers, a new, intermediate level of conductance was observed. By analogy with previous observations of hybrid channel formation with gramicidin analogues,^{37,54} this new level is ascribed to a hybrid channel formed by Pap¹-gA and gA monomers. Similar results were obtained when Pap¹-gA(trans) was mixed with native gA (data not shown). The conductance of hybrid Pap¹-gA(trans)/gA channels was a little

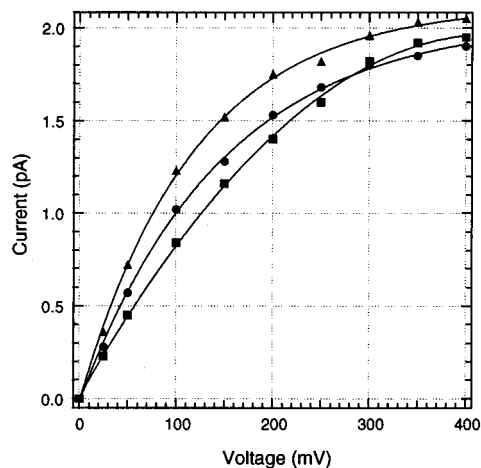


Figure 6. Single-channel current–voltage plots at low permeant ion concentration (0.1 M CsCl, 5 mM BES, pH 7; filtering was at 50 or 100 Hz). Pap¹-gA(cis/cis) (■), Pap¹-gA(trans/trans) (●), and native gA (▲).

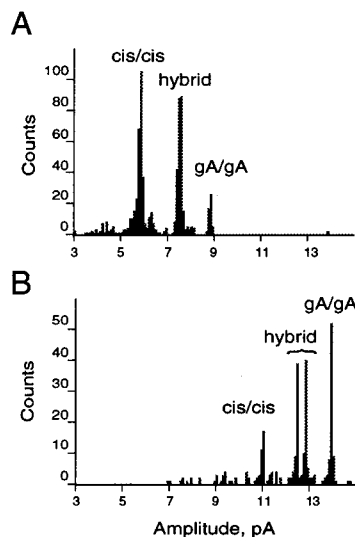


Figure 7. Current amplitude histograms of single channels obtained with a mixture of gA and Pap¹-gA(cis). (A) +200 mV applied potential. (B) +350 mV applied potential. 1.0 M CsCl, 5 mM BES, pH 7; filtering was at 100 Hz. Several hundred channels of each type were characterized.

higher than that of hybrid Pap¹-gA(cis)/gA channels which, in turn, was higher than that of Pap¹-gA(trans/trans) homodimers (Table 1).

Two different hybrid channels are expected to form, i.e. Pap¹-gA/gA and gA/Pap¹-gA, with opposite orientations with respect to the applied field. These may or may not exhibit different conductances, depending on the degree of asymmetry in the corresponding free energy profiles for cation movement and the size of the applied field.^{37,55} In the present case, no splitting of the hybrid peak is observed at 200 mV (Figure 7A), but splitting is observed at 350 mV (Figure 7B).

Current–voltage curves of gA/Pap¹-gA(cis) hybrid channels and gA/Pap¹-gA(trans) hybrid channels in 1 M CsCl (0–400 mV range) had shapes intermediate between those of the corresponding pure homodimers (not shown). The superlinearity of $I-V$ curves increased in the following order: gA/gA < gA/Pap¹-gA(trans) < gA/Pap¹-gA(cis) < Pap¹-gA(trans/trans) <

(52) Andersen, O. S. *Biophys. J.* **1983**, *41*, 119–133.

(53) Andersen, O. S. *Biophys. J.* **1983**, *41*, 135–146.

(54) Durkin, J. T.; Koeppe, R. E., II; Andersen, O. S. *J. Mol. Biol.* **1990**, *211*, 221–234.

(55) Andersen, O. S.; Durkin, J. T.; Koeppe, R. E., II. In *Transport through membranes: carriers, channels and pumps*; Pullman, A., Jortner J., Pullman, B., Eds.; Kluwer Academic: Dordrecht, 1988; pp 115–132.

Pap¹-gA(cis/cis). Average lifetimes of gA/Pap¹-gA(cis) and gA/Pap¹-gA(trans) hybrid channels were similar to those of homodimer channels (Table 1).

Discussion

Pap¹-gA Channels Have the Same General Architecture as Native gA Channels. Before considering the mechanism whereby photoisomerization of Pap¹-gA alters channel function, one must first determine whether a substantial change in the overall structure of the channel has occurred as a result of the introduction of the Pap group. A stringent test of the degree to which the channel structure has been altered by chemical modification is the ability of modified peptides to form heterodimers with native gA peptides.⁵⁴ If the structure of Pap¹-gA is exactly like that of gA, then one would expect no difference between the interaction energies of gA homodimers and gA/Pap¹-gA heterodimers. If there is no energetic difference, the following relationship should hold:^{37,54,56}

$$\phi_H/2(\phi_A\phi_B)^{1/2} \geq 1 \quad (1)$$

where ϕ_H is the frequency of appearance of hybrid channels (of either orientation), and ϕ_A and ϕ_B are the frequencies of appearance of gA and Pap¹-gA homodimer channels. When gA/Pap¹-gA(cis) hybrid channels were examined (Figure 7), the ratio $\phi_H/2(\phi_A\phi_B)^{1/2}$ was found to be 1.12 at 200 mV. For hybrid gA/Pap¹-gA(trans) channels, the ratio was 1.02. Both of these ratios are very close to 1, indicating that there is very little energetic difference between homo- and heterodimer channels. This result is strong evidence that the overall structure of the Pap¹-gA channel is the same as the native gA channel, that is, a β -helical dimer.⁵⁷

Trans-to-Cis Photoisomerization of Pap¹-gA Increases the Barrier for Alkali Cation Translocation. Since we are primarily interested in the effects of photoisomerization, we will focus on the conductance differences between Pap¹-gA(trans) and Pap¹-gA(cis) channels. However, we note there is also a difference in the conductance properties of Pap¹-gA(trans) and native gA channels. Koeppel and Andersen and colleagues^{36,56} have reported the channel properties of position 1 mutants in which valine was altered to phenylalanine and a series of substituted phenylalanine derivatives. If one considers the phenylazo group as a substituent of phenylalanine, the observed conductance of Pap¹-gA(trans/trans) (1 M NaCl) is consistent with the observed trends reported by Koeppel et al.^{36,56} The low-voltage conductance of Pap¹-gA(trans/trans) is 7 pS vs 10.2 pS for Phe¹-gA, 6 pS for *p*-F-Phe¹-gA, 3.9 pS for *p*-OH-gA, and 12.5 pS for gA (1 M NaCl).^{36,56} Most of these conductances could be rationalized by considering the projections of group moments of the side chains along the α - β bond. A similar analysis for Pap¹-gA(trans/trans) would presumably explain why the conductance of Pap¹-gA(trans/trans) falls in the middle of the observed range. However, since we were primarily interested in comparing cis and trans Pap¹-gA channels to one another, rather than to native gA, we chose to represent side-chain dipole moments using atom-centered partial charges as this proved more amenable for use with the molecular mechanics algorithms used for conformational analysis (vide infra).

An isolated *cis*-azobenzene group with χ_3 and χ_4 torsion angles near 55° (as observed in the crystal⁴⁵) has a dipole moment of approximately 3.0 D; the trans conformation, if

planar, is expected to have a zero dipole moment.²² We now consider the possible effects of the photocontrolled occurrence of this dipole on channel activity.

Alkali cations must pass through gramicidin channels by diffusing to the channel mouth and entering the channel, moving through the pore (translocation), and finally, exiting from the channel.^{19,51} An azobenzene group attached to position 1 of gramicidin is located in the central part of the membrane and would not be expected to have a significant impact on the process of ion entry. When ion entry is made the rate-limiting step, by having a low concentration of permeant electrolyte and a high applied voltage, no difference is observed in the conductance of cis and trans Pap¹-gA channels (Figure 6). Modified channels, where the modification is at the channel entrance (e.g., gramicidin–ethylenediamine²⁴), do not, in general, show this behavior.

In contrast, an azobenzene dipole at the center of the membrane might be expected to affect the translocation process. When translocation is made rate limiting by using 1 M NaCl or CsCl electrolyte solutions and diphytanoyl-phosphatidylcholine membranes,²⁶ conductance changes are seen upon photoisomerization of Pap¹-gA(trans) to Pap¹-gA(cis) (Figures 3 and 4). In addition, the shapes of the corresponding *I*–*V* curves are consistent with an increase in the barrier for alkali cation permeation when the Pap group isomerizes from trans to cis (Figure 5).

The effect of photoisomerization is more pronounced with NaCl than CsCl (Figures 3–5). This presumably reflects differences in the detailed free energy profiles for these ions; a similar pattern has been seen with other position 1 mutations that alter the dipole moment of the side chain.³⁶ Indeed, proton flux through the channel, which is expected to be governed by an entirely different free energy profile,^{29,58–60} was found to be almost unaffected by photoisomerization (Table 1).

Molecular Origins of the Effects of Photoisomerization on Conductance. If the photocontrolled introduction of a dipole at the center of the membrane is, indeed, responsible for the observed effects on alkali cation conductance, then the dipole must act in such a way as to increase the barrier for ion translocation. Taking the native gramicidin channel structure as determined by solid-state NMR as a starting point,⁵⁷ we performed energy calculations to identify conformations that would be available to a *cis*-Pap group at position 1 in the channel. We assumed that the χ_3 and χ_4 torsion angles (Figure 1) of the Pap group would be close to those observed in the azobenzene crystal.⁴⁵ Four pairs of χ_3 , χ_4 torsion angles are thus possible (enantiomeric forms of an isolated azobenzene become diastereomeric when attached to gramicidin). For each pair of χ_3 , χ_4 torsion angles, a systematic calculation of conformational energy versus the torsion angles χ_1 and χ_2 was carried out assuming the conformation of the rest of the molecule was unchanged. This simple search identified relatively restricted regions of the χ_1 , χ_2 map which were energetically allowed (Figure 8). These regions were determined almost entirely by van der Waals interactions, i.e. steric clashes, with other side chains.

For each value of χ_1 and χ_2 , we also calculated the electrostatic energy of interaction between the Pap dipole (represented by atom-centered partial charges) and a sodium

(58) Quigley, E. P.; Quigley, P.; Crumrine, D. S.; Cukierman, S. *Biophys. J.* **1999**, *77*, 2479–2491.

(59) Sadeghi, R. R.; Cheng, H. P. *J. Chem. Phys.* **1999**, *111*, 2086–2094.

(60) Schumaker, M. F.; Pomes, R.; Roux, B. *Biophys. J.* **1999**, *76*, A442–A442.

(56) Mazet, J. L.; Andersen, O. S.; Koeppel, R. E., II. *Biophys. J.* **1984**, *45*, 263–276.

(57) Kovacs, F.; Quine, J.; Cross, T. A. *Proc. Natl. Acad. Sci. U.S.A.* **1999**, *96*, 7910–7915.

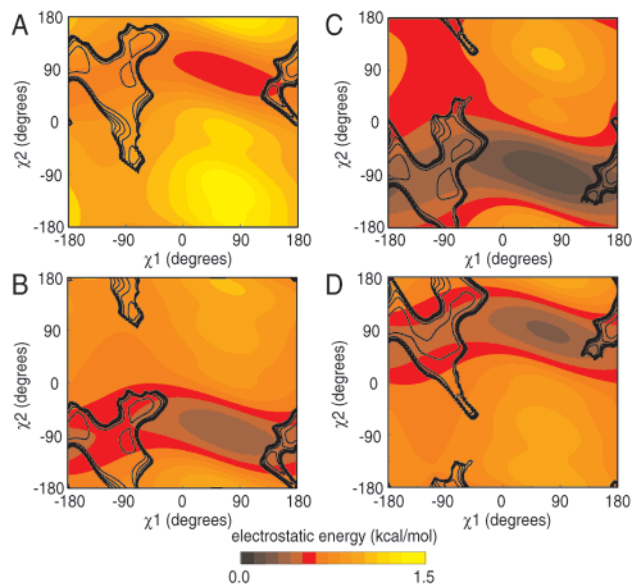


Figure 8. Conformational energy contours (dark lines) and electrostatic energies (shaded zones) as a function of torsion angles χ_1 and χ_2 in Pap¹-gA(cis/cis) for the four low-energy χ_3 , χ_4 conformers of *cis*-Pap: (A) χ_3 , $\chi_4 = -56.9^\circ$, (B) χ_3 , $\chi_4 = 123.1^\circ$, (C) χ_3 , $\chi_4 = 56.9^\circ$, (D) χ_3 , $\chi_4 = -123.1^\circ$. Conformational energy is lowest (~ 0 kcal/mol) for $\chi_1 \approx -90$ and $\chi_2 \approx +90$ (A,D) or -90 (B,C). Contours are drawn at 10 kcal/mol intervals; conformational energy is thus prohibitively high throughout most of the χ_1 , χ_2 map. The scale for the electrostatic interaction energies (shaded zones) between Pap partial charges and a sodium ion at the center of the channel is given at the bottom of the figure.

ion positioned at the center of the channel. Since we were primarily interested in whether the electrostatic interaction was favorable or unfavorable, we used a uniform dielectric constant, $\epsilon = 5$, reported by Hu and Cross³³ to correctly reflect the effects of Trp dipoles on gramicidin conductance, measured under conditions similar to those used here. A more sophisticated treatment would consider the influence of the dielectric boundaries of the system^{28,61} and the dynamics of the side chains on the magnitude of the interaction energy.⁶² Nevertheless, we found that throughout the conformationally allowed zones, and indeed for all values of χ_1 and χ_2 , the electrostatic energy of interaction was positive and varied between 0.2 and 1.5 kcal/mol (Figure 8), a value similar in magnitude, but opposite in sign, to those estimated by others for the energy of interaction between Trp dipoles and a cation in the channel.²⁸

If we assume that the electrostatic energy of interaction between a *trans*-Pap group (which has almost no dipole) and a sodium ion in the channel is zero, this conformational analysis indicates that a *cis*-Pap group would always be expected to increase the barrier to alkali cation movement via an electrostatic mechanism since the positive end of the side-chain dipole is always oriented toward the center of the channel (Figure 9). Since the two Pap groups in a (dimer) channel are approximately on opposite sides of the channel (Figure 9), we assume that their interactions with ions in the pore are independent and additive. The finding that the conductances of heterodimer channels (which contain one Pap group) are intermediate between native gramicidin channels and homodimer Pap channels supports this assumption, i.e., that the two Pap groups act independently and additively. Given these assumptions, this simple electrostatic analysis suggests that photoisomerization

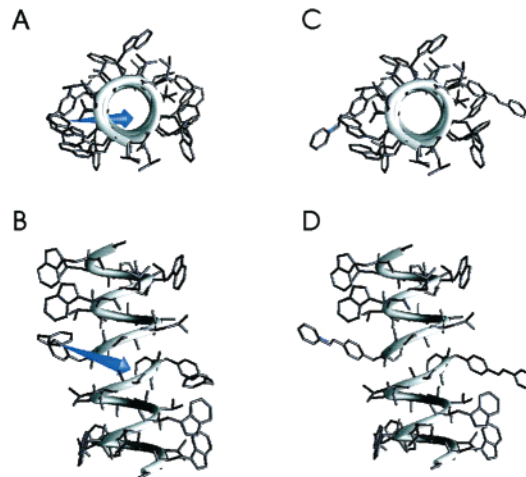


Figure 9. (A) Top view and (B) side view of Pap¹-gA(cis/cis) gramicidin. One low-energy conformer ($\chi_1 = 180.0^\circ$, $\chi_2 = -90.0^\circ$, $\chi_3 = 56.9^\circ$, $\chi_4 = 56.9^\circ$) of Pap¹ is shown. The azobenzene side-chain dipole of one Pap group is represented as a vector (arrowhead at the positive end) projecting into the channel lumen (drawn at a scale of 0.06 D/Å with the origin of the vector at the center of the actual dipole). (C) Top view and (D) side view of Pap¹-gA(trans/trans) ($\chi_1 = 180.0^\circ$, $\chi_2 = -90.0^\circ$, $\chi_3 = 0^\circ$, $\chi_4 = 0^\circ$).

of Pap¹-gA(trans/trans) to Pap¹-gA(cis/cis) would result in an increase in the central barrier by about 0.4–3 kcal/mol (0.2–1.5 kcal/mol for each Pap). The observed decrease in conductance (Figure 3, Table 1) indicates a change in barrier height of about 0.2 kcal/mol (for Na⁺), close to the low end of this calculated range. Thus, photoswitching of ion dipole interactions can, semiquantitatively, account for the observed effects on conductance. The overestimation of the electrostatic contribution may reflect the simplicity of the model (e.g., the fact that the discontinuous dielectric is neglected), or that other molecular details play a role. For instance, lipid packing might be expected to be significantly different around the *cis* and *trans* conformations (Figure 9).

With the present configuration, the sizes of the effects of photoisomerization are probably not large enough to permit Pap¹-gA to be of use for manipulating cellular excitability. The photomodulated properties of Pap¹-gA may be of use, however, for resolving gramicidin-associated currents from background currents in the gramicidin-based biosensor described by Cornell and colleagues.^{63,64} The predictability of the system does suggest that larger dipole changes or changes closer to the central axis of the pore could effect substantially larger changes in conductance. Compounds that undergo larger dipole moment changes upon photoisomerization such as spiropyran/merocyanine-based compounds could be substituted for azobenzene in the channel. Strategies for increasing the effects of photoisomerization on channel conductance might also include the use of conformationally restrained azobenzene analogues to control the orientation of the side-chain dipoles.⁶⁵

Acknowledgment. We thank NSERC Canada for financial support.

JA000736W

(63) Woodhouse, G.; King, L.; Wiczorek, L.; Osman, P.; Cornell, B. *J. Mol. Recognit.* **1999**, *12*, 328–334.

(64) Cornell, B. A.; Braach-Maksyvytis, V. L.; King, L. G.; Osman, P. D.; Raguse, B.; Wiczorek, L.; Pace, R. *J. Nature* **1997**, *387*, 580–583.

(65) Zhang, J.; James, D. A.; Woolley, G. A. *J. Pept. Res.* **1999**, *53*, 560–568.

(61) Martinez, G.; Sancho, M. *Eur. Biophys. J.* **1993**, *22*, 301–307.

(62) Woolf, T. B.; Roux, B. *Biophys. J.* **1997**, *72*, 1930–1945.